J. KAPRA Vol. 9, E. (1993) pp.347-357

Predicted Air Flow Around Objects Using the Discrete Vortex Method

Tae-Hyeung Kim

Department of Environmental Engineering
Changwon National University
(Received 2 August 1993)

Abstract

The Lagrangian grid-free numerical method, the discrete vortex method, was applied to solve the Navier-Stokes equations. This method avoids the introduction of numerical viscosity swamping the real physical viscosity at high Reynolds number, unlike Eulerian method, e.g. finite difference and element methods. The boundary integral equation method for the potential flow solution was included to make the discrete vortex method more feasible for complex geometries. The fast adaptive multipole expansion method was incorporated to reduce the computational time from $O(N^2)$ to O (N) for the computations of vortex-vortex interactions. The test problems were air flow around one circular cylinder and two circular cylinders in tandem with various gaps. The numerical results were in excellent agreement with the experimental and other computational results. The applicabilty of the method was discussed with the indoor and the outdoor air pollution problems, especially the contaminant transport in the recirculation regions.

1. INTRODUCTION

In the last decade, many empirical and numerical approaches have been taken in attempting to predict air flow around bluff bodies (Hunt and Castro, 1984;Wilson, 1982;Heinsohn, 1991;Okajima, 1990;Kim and Flynn, 1991a, b). Among others, a promising numerical tool is the discrete vortex method (DVM). Turfus (1988) used the DVM along with the particle trajectory method to study contaminant transport in the recirculation region behind a two-dimensional backward-facing step. Flynn and Miller (1991) used a similar method to predict a worker's breathing zone concentration in a uniform free-stream by assuming a worker as an elliptic cylinder.

This discrete vortex method has been used to co-nstruct numerical solutions for the Navier-Stokes equations at high Reynolds numbers (Leo-naonard, 1980). Its main features are as follows:(Chorin, 1980 ; Sethian, 1984) (i) the nonlinear terms in the Navier-Stokes equations are taken into account by the inviscid interactions among vortices of small but finite core, " vortex blob" , (ii) viscous diffusion is taken into account by adding to the motion of vortices a random Gaussian component of appropriate variance, (iii) no-slip boundary conditions are approximated by a vorticity creation algorithm, (iv) normal boundary conditions are met through the addition of a potential flow solution.

The advantage of this method is two-fold. First, this Lagrangian approach avoids the introduction of numerical viscosity swamping the real physical viscosity since no grid is introduced unlike the Eulerian approach, e.g., finite differ-

ence and element methods. Second, this method is dynamically adaptive since computational elements are naturally clustered in regions of large flow gradients where accuracy is required.

On the other hand, it requires the excessive computational labor to compute the vortex-vortex interaction at each time step, as the number of vortex elements is increased. Given N vortex elements, computing the velocity at each of N vortex elements requires $O(N^2)$ operations, which is known as an 'N-body problem'. Various techniques have been developed to reduce the operation counts from $O(N^2)$ down to O(N). A most promising technique is the fast adaptive multipole expansion algorithm by Carrier et. al..(1988) The second big computational labor involved in this method is to compute the velocity due to a potential flow at each time step. Analytical solutions to this problem are possible for certain geometries, involving the use of the method of images. For some geometries it is necessary to use conformal mapping before the method of images can be applied. The principal alternative, cheap and flexible, to the image system for a complex geometry problem, is the boundary integral equation method involving a fixed array of external singularities based on Green's second identity (Ligget and Liu, 1983).

In this paper, discrete vortex computer models were developed to solve the 2-D Navier-Stokes equations for the time dependent air flow around a circular cylinder and two circular cylinders in tandem with various distances in a uniform freestream. Both the boundary integral equation method and the fast adaptive multipole expansion algorithm were implemented to make the discrete vortex method more feasible for complex engineering problems. The computational results were compared with experimental/ computational ones. The applicability of this approach was extensively discussed in conjunction with a worker exposure problem in workplace.

2. NUMERICAL METHODS

2.1 DISCRETE VORTEX METHOD

The governing equations for two-dimensional incompressible flow in vorticity form are

$$\frac{\partial \xi}{\partial t}+(U+\nabla)\xi=\frac{1}{R}\nabla^2\xi \tag{1}$$

$$\nabla^2\Psi=-\xi \tag{2}$$

$$u=\frac{\partial \Psi}{\partial y},\ v=-\frac{\partial \Psi}{\partial x} \tag{3}$$

where $U=(u,v)$ is the velocity field, $\xi=\nabla\times U$ is the vorticity, t represents the time, Ψ is the stream function, and R is the Reynolds number. The boundary conditions are

$U\cdot\tau=0$ on the boundary ∂D, τ tangent to ∂D.

$U\cdot n=0$ on the boundary ∂D, n normal to ∂D.

The above system of equations can be splitted into two parts : an inviscid and a viscous part, respectively

$$\frac{\partial \xi}{\partial t}+(U\cdot\nabla)\xi=0 \tag{4}$$

and

$$\frac{\partial \xi}{\partial t}=\frac{1}{R}\nabla^2\xi \tag{5}$$

The Equation (4) and (5) are Euler (convection) equation and the diffusion equation, respectively.

The discrete vortex method, developed by Chorin (1973), relies upon the fact that vorticity is a material property of the fluid that is convected and diffused. The solution for Euler equation depends on a theorem (Batchelor, 1967) that guarantees, for incompressible flow, that a given velocity field may be decomposed into the sum of a potential flow and a rotational flow. The potential flow can be generated by a potential flow solution technique that will be discussed later. The rotational flow is generated by inviscid interactions between vortex blobs of small compact support. The solution for the diffusion equation is a Gaussian distribution of zero mean and of variance :

$$\sigma^2=\frac{2\Delta t}{R} \tag{6}$$

As air flows around objects, vorticity is generated by the action of viscosity in the boundary

layer. In order to mimic the physical problem, Chorin (1973) developed the concept of a numerical boundary layer governed by the Prandtl boundary layer equations. Within the boundary layer, vortex sheets are formed to cancel the tangential velocity at selected generation points on the surface of objects. The equations which govern the flow in the numerical boundary layer are:

$$\frac{\partial \xi}{\partial t}+(U \cdot \nabla)\xi=\frac{1}{R}\frac{\partial^2 \xi}{\partial y^2} \tag{7}$$

$$\xi=\frac{\partial u}{\partial y} \tag{8}$$

$$\frac{\partial u}{\partial x}+\frac{\partial v}{\partial y}=0 \tag{9}$$

with boundary conditions

$$U=(u,v)=(0,0) \qquad \text{at } y=0$$

$$u(x,y=\infty)=u_\infty(x)$$

In this set of equations, u and v refer to the velocity component in the tangential and normal directions to the boundary respectively. Similarly x and y refer to the tangential and normal directions to the boundary respectively.

To approximate this set of equations numerically, the equations are once again splitted into an inviscid and a viscous part :

$$\frac{\partial \xi}{\partial t}+(U \cdot \nabla)\xi=0 \tag{10}$$

$$\frac{\partial \xi}{\partial t}=\frac{1}{R}\frac{\partial^2 \xi}{\partial y^2} \tag{11}$$

The inviscid part of the equation is modeled using vortex sheets and the viscous part is modeled using random walks. For more details about this method, see reference (Cheer, 1983 ; Tiemroth, 1986 ; Bui and Oppenheim, 1987 ; Flynn and Miller, 1991).

2.2 BOUNDARY INTEGRAL EQUATION METHOD

As earlier mentioned, a given velocity field can be decomposed into the sum of a potential flow and a rotational flow. The potential flow can be then generated by solving Laplace equation. The boundary integral equation method (BIEM) is a cheap and flexible technique that can be used to solve the equation in a closed domain (D), in either two or three dimensions. It has the advantage of reducing the dimension of problem by its construction, thus leading this technique more feasible for complicated engineering problems.

The final form of the BIEM solution to Laplace equation is given as follows :

$$\alpha\Phi(P)=\int_{\Omega}\left[\frac{\Phi}{r}\frac{\partial r}{\partial n}-\ln r\frac{\partial \Phi}{\partial n}\right]ds \tag{12}$$

where α is the angle between the boundary segments at the singular point, Φ is the velocity potential, Ω is the boundary of the domain D, r is the the distance between the singular point and another point on the boundary of the domain, and n is the unit outward normal to D on Ω A complete discussion can be found in Ligget and Liu (1983) and Brebbia and Dominguez (1989).

The numerical procedure involves selecting a finite number (N) of boundary points and performing the line integrations defined in Equation (12). By sequentially moving from one boundary point to the next and properly partitioning the coefficients, a system of N equations in N unknowns results. Here the coefficient matrix is constant as long as the physical boundary is not changed, allowing for the use of an efficient lower-upper decomposition solver. Solution of this system gives both potential and velocity normal to the boundary at each node on the boundary. With this information, one can move to the interior of the domain and differentiate Equation (12) with respect to the coordinates to obtain velocities at internal points.

In this study, a FORTRAN computer code (GM8.FOR) from Ligget and Liu (1983) was adopted. This code was written for a problem with one connected boundary. It was modified to solve Laplace equation with more than one boundary. The modified code was successfully validated with the analytic solutions (Lamb, 1945) for a flow around an ellipse.

2.3 FAST ADAPTIVE MULTIPOLE ESPANSION METHOD

In the application of the discrete vortex method, the bulk of the computational burden at each time step is the evaluation of all pairwise interactions of N vortex blobs which, by direct summation, requires $O(N^2)$ work. Several authors have investigated fast summation algorithms to lower the operation count.

A straightforward approach, continuum method, is to solve directly for the stream function by introducing a finite-difference grid. Then the discrete vorticity field is interpolated to neighboring grid points, and a fast Poisson solver is used to find the stream function at grid points. This 'vortex-in-cell' technique (Christiansen, 1973 ; Baker, 1979) has an operation count O(NlogN), but introduces significant inaccuracy into the computation of vortex interaction. Another approach, hierarchical method, uses fast solvers for the contributions of far away effect, and direct summation for the nearby elements(Greengard and Rokhlin, 1987 ; Barnes and Hut, 1986)

The fast multipole method shares certain characteristics with the hierarchical solvers. Tree structures are imposed to partition space uniformly, and the strategy is similar, but analytic observations concerning multipole and Taylor expansions are used to produce results that are accurate to within round-off error. The CPU requirements are of the order $O(N \log(1/\varepsilon))$, where ε is the desired accuracy. This method was applied in computational fluid dynamics using the discrete vortex method (Anderson, Greengard, Greengard, and Rokhlin, 1990). Unfortunately the performance of the method was not discussed.

Recently, an adaptive version of the above method, 'fast adaptive multipole method', was developed by Carrier et. al. (1988) to speed up the computations and reduce the storage requirement. It does not use the same number of subdivision levels for all parts of the computational domain. Instead, some integer $s>0$ is fixed, and at every level of refinement the boxes containing more than s particles are subdivided. By noting that, in the discrete vortex method, computational elements are naturally clustered in regions of large flow gradients, this adaptive version may be the best with the discrete vortex method.

3. NUMERICAL SIMULATIONS

3.1 ONE CIRCULAR CYLINDER

Initially, a flow around a two-dimensional circular cylinder started impulsively from rest was selected as a validation problem. This problem was used by many authors with different numerical methods. Among others, Cheer (1983) used the discrete vortex method along with the image method for the potential flow. Her results were successfully validated with experimental results.

The boundary of the circle was divided into $M=20$points with the same arc length $h=\pi/M$, at which the tangential velocity is computed and the vortex sheets are generated to cancel the tangential velocity. The diameter of the circle, D, was equal to 1. The Reynolds number was 2000. The boundary points for the boundary integral equation method, 40 and 20, were assigned on the boundary of the circle and the square respectively. The square of 300 unit length with the same center as that of the circle was served as the outside boundary. Through this outside boundary, the external boundary conditions, e.g. flow velocity and direction, can be incorporated. The cut-off value for the vortex blob, δ, was equal to h/π which has been shown(Cheer,1983) asan appropriate value permitting fast convergence and smooth transition from sheets to blobs. The maximum tolerable sheet strength, ξ_{max}, was 0.25. After computing the tangential velocity (u_t) at each generation point, no sheet was generated on the point of its u_t less than ξ_{max}. Otherwise u_t was evenly divided by N, where N is the integer part of u_t/ξ_{max}.

The size of time step, t, is an important parameter, where t was measured in nondimensional units ($t=t^*U/D$, U=freestream velocity). Here the most well known and the only universally acknowledged condition on parameters is

$$\Delta t\, U_{max} \leq h$$

where U_{max} is the maximum tangential velocity

on the physical boundary of the object. This requirement ensures that no sheet is advected downstream a distance greater than its length during one time step. Although Cheer's Δt of 0.2 is somewhat large based on U_{max} of 1.9 with the unit freestream velocity, the same value was temporarily used. The flow was simulated up to the nondimensional time t=11, resulting 55 time steps.

The criteria for the numerical boundary layer thickness (NBLT) was suggested (Sethian, 1984 ; Chorin, 1980) based on the following reasons. The NBLT should be $O(R^{-1/2})$, which is the order of the physical boundary layer thickness. In addition, the NBLT should be taken as a multiple of σ, the standard deviation of random walk, to minimize the loss of vortex blobs due to random walk. Sethian et. al. (1990) suggested the NBLT of 2σ with the statement 'some experimentation is possible to find an equitable balance between sheets and blobs.' The procedure of metamorpho-sis in this work is little different from that in Sethian et. al.'s work (1990). If a blob goes into the imaginary numerical boundary, which has the same thickness but is inside the wall, the blob will be reflected as a sheet. If it goes further inside, it will be removed. On the other hand, in Sethian's procedure, whenever a blob penetrate the wall, it will be removed. Thus the NBLT of σ is equivalent to 2σ in Sethian's work to have the same probability to lose blobs.

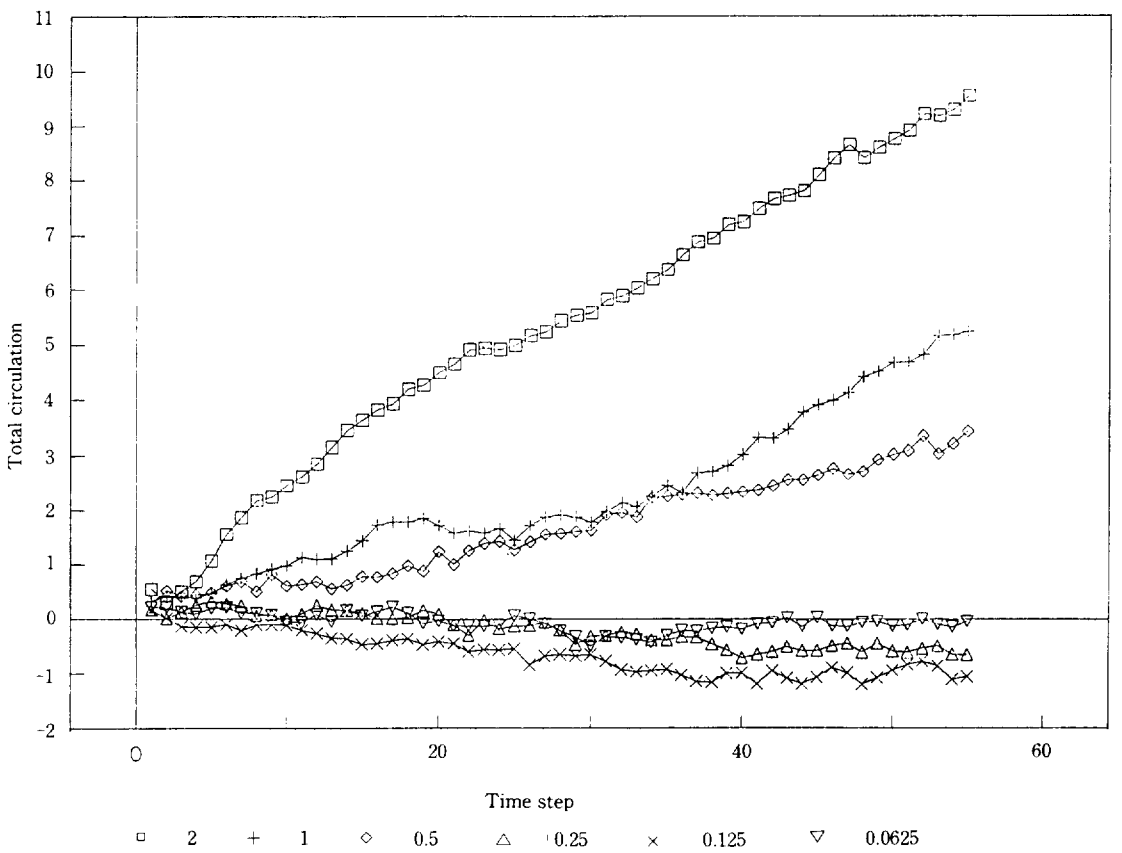

Fig. 1. Total circulation with different numerical boundary layer thickness

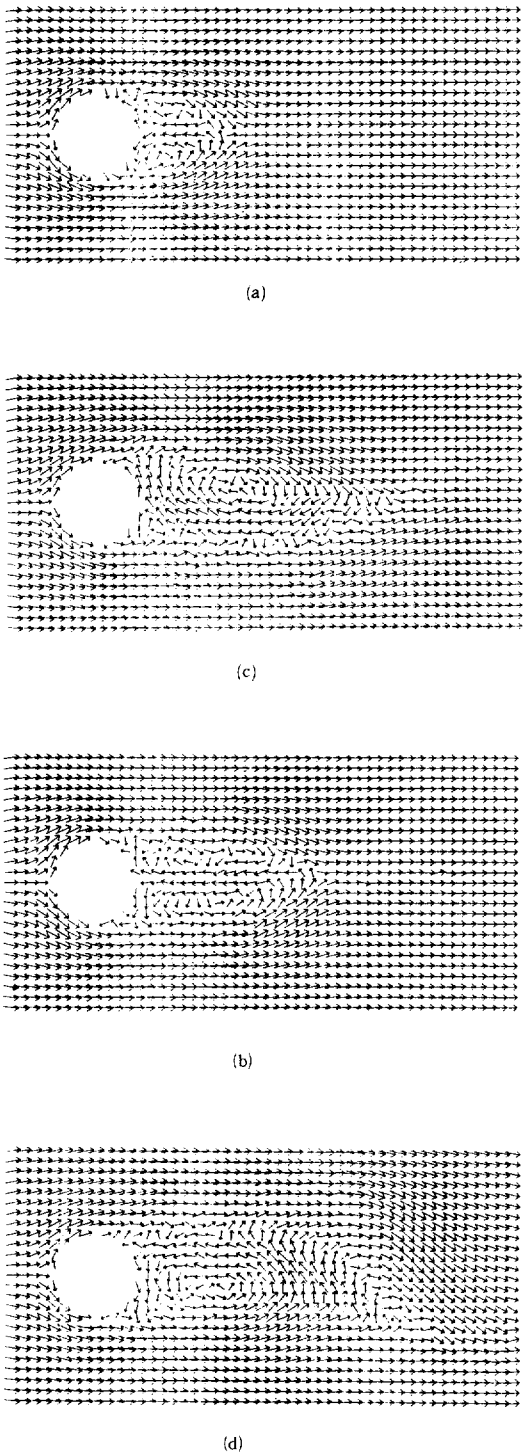

Fig. 2. Air flow around a circular cylinder at t= (a)2, (b)5, (c)8, and (d) 11

The numerical simulations were performed with the various NBLTs while the total circulation was monitored at each time step. The total circulation was calculated by summing the circulation of all vortex elements. In the theoretical sense, the total circulation of the test problem is supposed to be 0, because of the symmetry. As shown in Figure (1), the absolute total circulation grows faster with the thicker NBLT. With the thicker NBLT, in general, the flow upstream of the cylinder was not symmetric but more skewed due to the larger total circulation. This kind of skewness was exaggerated for the problem with the weaker separation points, e.g. a uniform flow around an ellipse of its major axis parallel to the freestream. To my knowledge, nobody reported the dependence of the solutions on the NBLT, except for the above Sethian's statement. We suspect that it was caused by the inaccuracy of the boundary integral equation method near the boundary. Nevertheless, the solutions with the thinner NBLT ($0.125\times 2\sigma$), as shown in Figure (2), were comparable with Cheer's results. The similar solutions were obtained with the NBLTs of $0.25\times\sigma$ and $0.0625\times\sigma$. It took less than 1.5 min. of CPU-time on Convex C220 mid-range supercomputer. At time t=11, the flow was modeled by approximately 800 computational elements.

The longer time simulations were subsequently conducted to further validate with one circular cylinder problem and to prepare for the next step, i.e. two circular cylinders in tandem with various gaps. In stead of comparing the flow pattern for a short simulation, the vortex shedding frequencies (f) were here obtained. The nondimensional vortex shedding frequency,

$$\frac{fD}{U}=S$$

is known as the Strouhal number where D is the diameter of the circular cylinder and U is the free-stream velocity. The value of S is constant at 0.19–0.21 (Schlichting, 1979) in the range of Reynolds numbers from 400 up to 2×10^5. The velocity signals in the freestream direction were monitored at points on the lines 1 and 3 diameters downstream of the cylinder center. Each line has

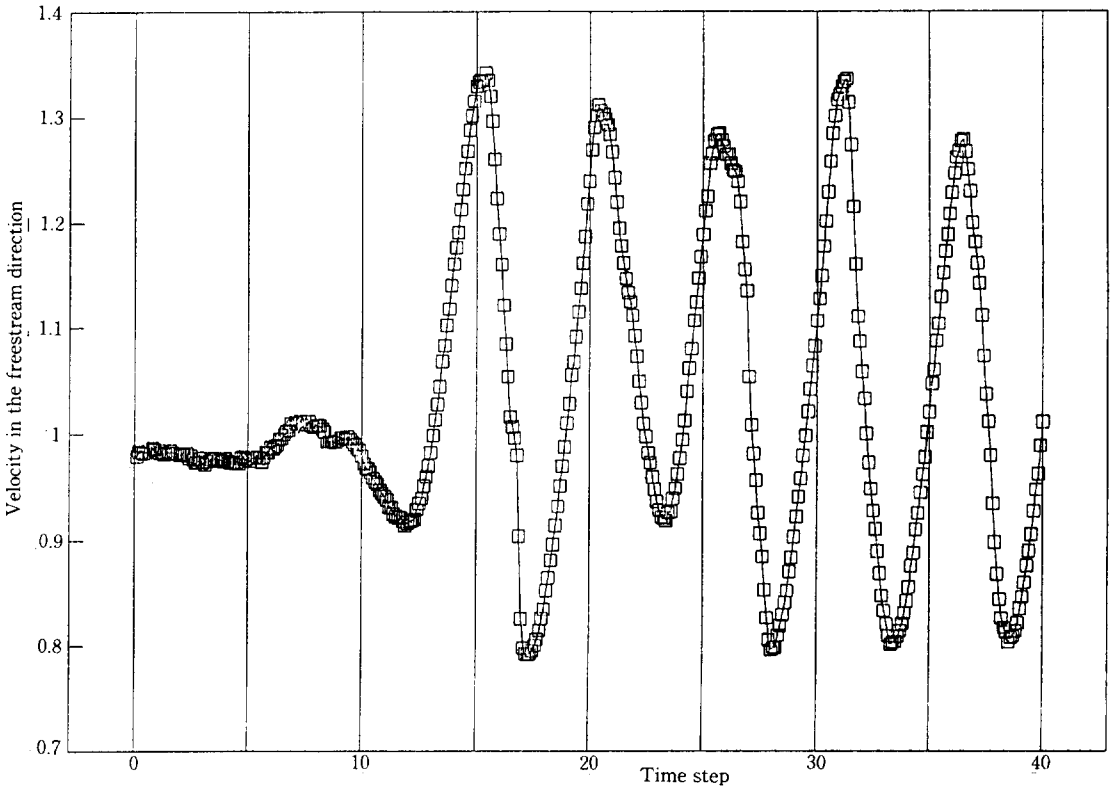

Fig. 3. Velocity signals downstream of the circular cylinder.

6 points -1.5, -1.0, -0.5, 0.5, 1.0, and 1.5 radii from the centerline, total 12 monitoring points with 3 points in each side on each line. The signals on the 3 monitoring points in each side were collectively plotted on one graph. After comparing three lines of the signals, it was easy to discern whether the strange jumps in the signals is due to the position of the monitoring point, since the signals on one monitoring point were sometimes not regular while the signals on other points had a regular pattern, especially when the monitoring point is near the center of eddy.

All the numerical parameters were kept the same as before except for R=13000. Then it was simulated up to t=40, requiring 200 time steps with $\Delta t=0.2$. As pointed out before, $\Delta t=0.2$, which Cheer (1983) used, was somewhat large. It resulted S=0.15-0.17 lower than expected. In fact, Cheer used the shorter Δt, 0.03-0.005, in her later paper (1983). Then t was reduced to 0.1, resulting 400 time steps. It took about 113 min. CPU-time on Convex C220 with 4659 computational elements at the final time step. As illustrated in Figure (3), the Strouhal number was about 0.19 which is in good agreement with the experimental results.

3.2 TWO CIRCULAR CYLINDERS IN TANDEM WITH VARIOUS GAPS

Subsequently, the simulations were performed for air flow around two circular cylinders in tandem with various gaps. The upstream and downstream cylinders arranged in a unit freestream with the gap, L, the distance between the centers of the cylinders. The four different gaps, 1.91, 2.5, 3.09 and 3.82 diameters, were chosen to compare with Igarashi's (1981) experimental Strouhal numbers of downstream cylinder and flow patterns.

The modification of the code for one cylinder required the addition of one more cylinder, the resulting change of potential solver, and the more

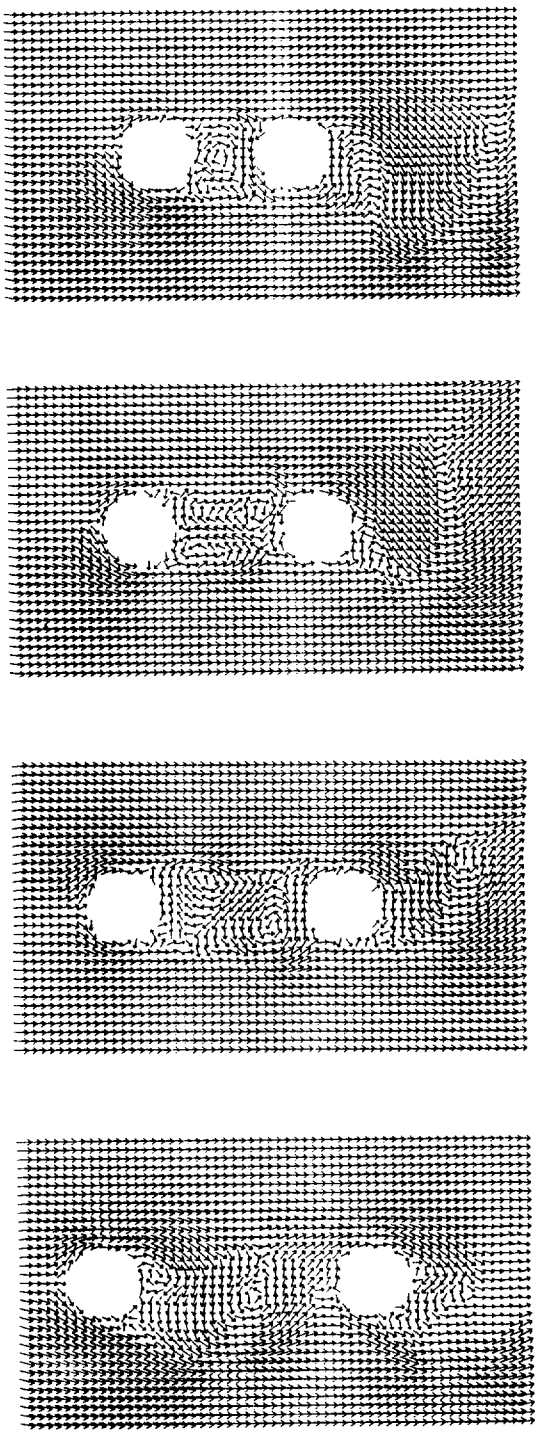

Fig. 4. Flow around two circular cylinders with L/D=(a) 1.91, (b) 2.5, (c) 3.09, and (d) 3.82

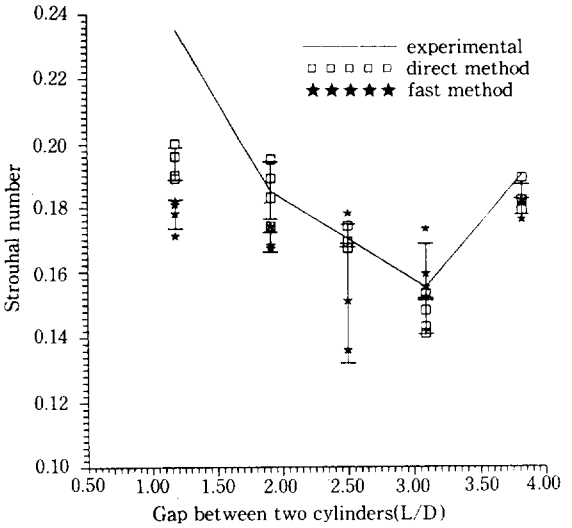

Fig. 5. Comparison of Strouhal numbers.

complicated metamorphosis and data structure. The numerical parameters were kept the same as those used in the later part of one cylinder problem. Again the velocity signals were monitored for the downstream cylinder in the same manner as that in one cylinder case.

The instant velocity profiles were demonstrated in Figure (4), L/D=1.91, 2.5, 3.09, and 3.82, respecti-vely. Up to L/D=2.5, the flow between two cylinders forms the closed circulation bubble, that is, not much interactions with the external flow. It is interesting to see the eddies inside the bubbles, while it may be difficult to catch the detailed flow with the experimental techniques, e.g. smoke visualizations. At L/D=3.09, the external flow starts to cross the wake axis, especially at upstream side of the downstream cylinder. Finally, at L/D=3.82, the external flow crosses the wake axis more completely and the vortex street was formed in between two cylinders. These flow patterns are very similar to Igarashi's flow visuali-zation results. In addition, the Strouhal numbers for the downstream cylinders were obtained in the same manner as above. As shown in Figure (5), they were compared with the experimental results, showing a good agreement except for the closest gap, L/D =1.18. It may be too close to detect the phenomenon!

Until now, all computations were performed with the direct summation of vortex elements, which requires $O(N^2)$ evaluations. The code for the fast adaptive multipole expansion method was obtained from Dr. L. Greengard, and was little modified to adjust for our problems since his code was written for evaluating the electric potentials and fields. It was tested with a sample set of vortex elements to see the accuracy of the method. The test was successful with a lot shorter CPU-time requirement, O(N). The direct method was replaced with the fast method in the two cylinder code. The Strouhal numbers were obtained, as shown in Figure (5). The results were a little different from those by the direct method. Since the discrete vortex method has the stochastic nature due to the random walk representation of diffusion, the subsequent simulations at L/D=1.91 were performed with three different seed numbers. The results showed that two identical simulations with the different seed numbers could result in about the same difference of the Strouhal number between two methods. Additionally, the cumulative CPU-time requirements of two codes using different summation method were compared in Figure (6). It shows one-third of CPU-time requirement with the fast method over the code with the direct method. Even if the CPU-time requirement is O(N) only with the vortex summations, there are some other portions requiring more than O (N), e.g. the potential solver, the vortex sheet algorithm.

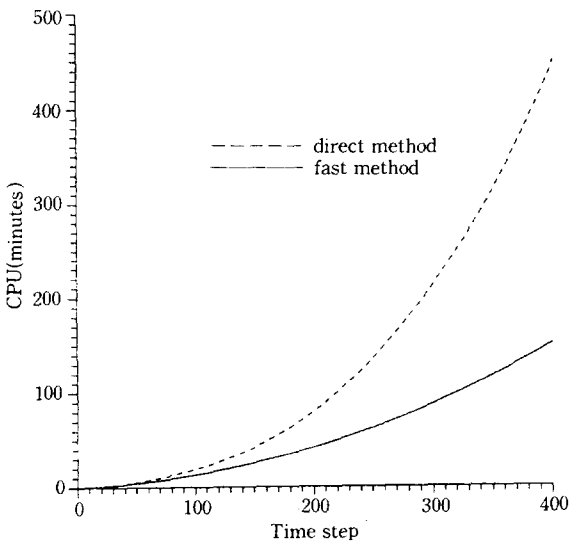

Fig. 6. Comparison of CPU-time requirement: direct vs. fast method.

4. APPLICABILITH OF THE DISCRETE VORTEX METHOD

The numerical results in the above section showed the excellent agreement with the experimental results. Moreover, it showed the possibility of making the discrete vortex method more feasible for engineering problems by using the more flexible and faster potential solver (the boundary integral equation method) and the fast summation technique (the fast adaptive multipole expansion method).

With these improvements, it was applied to air flow around an ellipse and a square with two different freestream directions. These configurations could be the simplification of the situations, i.e., the velocity field around a worker in close proximity to an obstacle (workpiece) in a booth type hood. The instantaneous velocity fields are illustrated in Figures (7) and(8). Figure(7) illustrates the velocity field when workers position a workpiece between themselves and the source of local exhaust, i.e. the typical orientation. In this case, the strong recirculating flow downstream of the workermay lead the over-exposure when the contaminant source is located in between the worker and the workpiece. On the other hand, Figure (8) shows the velocity field of a different orientation, only with the worker to the side of the workpiece. The weaker recirculation zone was formed not in front of worker, but at the side of the worker. thus the

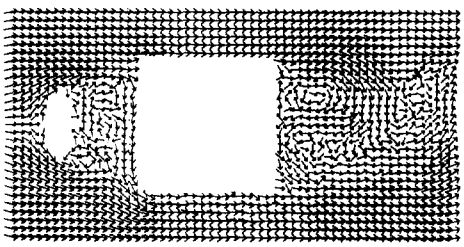

Fig. 7. Air flow around an ellipse and a square.

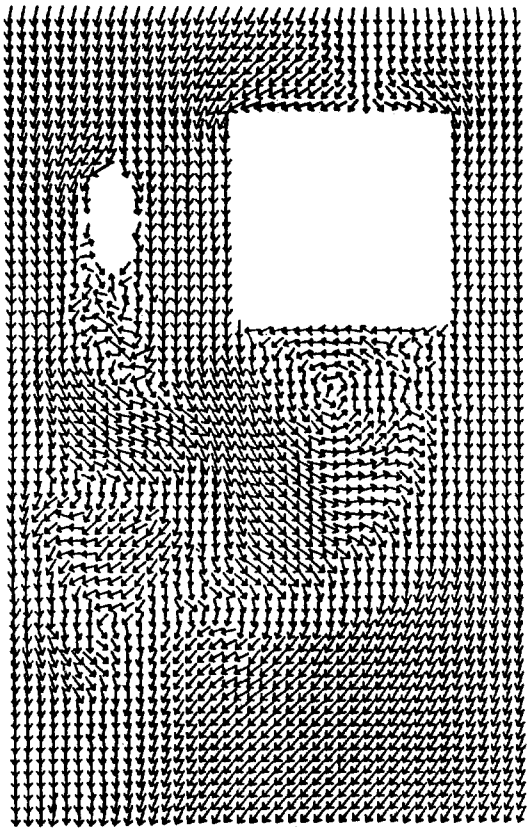

Fig. 8. Air flow around an ellipse and a square.

latter orientation may prevent the over-exposure. Or it could be applied to micro-scale air pollution problems near the buildings, e.g. the higher ground level concentrations of contaminants from a short stack in the building complex.

Along with this flow prediction technique, the particle trajectory method can be used to predict the concentration of 'neutrally buoyant' contaminants. By introducing massless tracer particles following the air flow, the concentrations of contaminant can be easily estimated with an appropriate weighting factor, based on the Lagrangian integral time scale, the eddy diffusivity, the ages of particles, etc.. Turfus (1988) first applied this technique to contaminant transport in the recirculation region behind a two-dimensional backward-facing step. The advantages of the technique was presented in the paper, over a diffusion equation method for dealing with dispersion in inhomogeneous flow. Chen (1992) later applied the technique to the problem similar to those in Figures (7) without the square. The results were compared with those from the tracer gas method using an anthromorphic mannequin. The breathing zone concentrations of worker were compared, resulting the factor 2-3 difference even though a strong three-dimensional convective flow existed in the experiment. The applications of 3-D discrete vortex method is presently underway.

5. CONCLUSIONS

The two-dimensional discrete vortex method was applied to air flow around one circular cylinder and two circular cylinders in tandem with various gaps. The flow patterns and Strouhal numbers were comparable with the experimental results. The more feasibility was added to the engineering applications of the method by including the boundary integral equation method for the potential flow solutions and the fast adaptive multipole method for the computations of the vortex-vortex interactions. This method can be applied to various indoor and outdoor air pollution problems with the particle trajectory method. On the other hand, some open questions regarding the dependence of the solutions on the numerical boundary layer thickness, remain to be answered by analysis or more computations.

ACKNOWLEDGMENTS

This work is supported by the U.S. National Institute for Occupational Safety and Health, Grant 5 R01 OH02392-02. The author wish to thank Dr. L. Greengard for providing his fast adaptive multipole code.

REFERENCES

Anderson C. R., Greengard C., Greengard L., Rokhlin V. (1990) On the accurate calculation of vortex shedding. Phys. Fluids A 2 (6), 883~885.

Baker G. R. (1979) The cloud-in-cell technique applied to the roll up of vortex sheets. J. Comput. Phys. 31, 76~95.

Barnes J. and Hut P. (1986) A hierachial O(N log N) force calculation algorithm. Nature 324, 446~449.

Batchelor G. K. (1967) An Introduction to Fluid Dynamics. Cambridge University Press, Cambridge, U. K.

Brebbia C. A. and Dominguez J. (1989) Boundary Elements;An Introductory Course.

Bui T. D. and Oppenheim A. K. (1987) Evaluation of wind effects on model buildings by the random vortex method. Appl. Numer. Math. 3, 195~207.

Carrier J., Greengard L., Rokhlin V. (1988) A fast adaptive multipole algorithm for particle simulations. SIAM J. Sci. Stat. Compt. 9(4), 669~686.

Cheer A. Y. (1983) Numerical study of incompressible slightly viscous flow past blunt bodies and airfoils. SIAM J. Sci. Stat. Comput. 4, 685~705.

Cheer A. Y. (1983) Unsteady separated wake behind an impulsively started cylinder in slight viscous fluid. J. Fluid Mech. 201, 485~505.

Chen M. M. (1992) Computational simulation of worker exposure using a particle trajectory method. Master Thesis, University of North Carolina, Chapel Hill, North Carolina, U.S.A.

Chorin A. J. (1973) Numerical study of slightly viscous flow. J. Fluid Mech. 57, 785~796.

Chorin A. J. (1980) Vortex models and boundary layer instability. SIAM J. Sci. Stat. Comp. 1, 1~21.

Christiansen J. P. (1973) Numerical simulation of hydrodynamics by the method of point vortices. J. Comput. Phys. 13, 363~379.

Flynn M. R. and Miller C. T. (1991) Discrete vortex methods for the simulation of boundary layer separation effects on worker exposure. Annals of Occupational Hygiene 35 (1), 35~50.

Greengard L. and Rokhlin V. (1987) A fast algorithm for particle simulations. J. Comput. Phys. 73, 325~348.

Heinsohn R. J. (1991) Industrial Ventilation : Engineering Principles, John Wiley & Sons, Inc., New York, U.S.A.

Hunt A. and Castro I. P. (1984) Scalar dispersion in model building wakes. Journal of Fluid Mechanics 73, 453~464.

Igarashi T. (1981) Characteristics of the flow around two circular cylinders arranged in tandem. Bull. JSME, 24(188), 323~331.

Kim T. H. and Flynn M. R. (1991a) Airflow pattern around a worker in a uniform freestream. Am. Ind. Hyg. Assoc. J. 52(7), 287~296.

Kim T. H. and Flynn M. R. (1991b) Modeling a worker's exposure from a hand-held source in a uniform freestream. Am. Ind. Hyg. Assoc. J. 52(11), 458~493.

Lamb H. (1945) Hydrodynamics, Dover, New York, U.S.A.

Leonard A. (1980) Review : Vortex methods for flow simulation. J. Comp. Phys. 37, 289~335.

Ligget J. A. and Liu P. L-F (1983) The Boundary Integral Equation Method for Porous Media Flow, George Allen & Unwin, London, U.K.

Okajima A. (1990) Numerical simulation of flow around rectangular cylinders. Journal of Wind Engineering and Industrial Aerodynamics 33, 171~180.

Schlichting H. (1979) Boundary-Layer Theory. McGraw-Hill, New York, U.S.A.

Sethian J. A., Brunet J-P, Greenberg A., Mesirov J. P. (1990) Two-dimensional, Viscous, Incompressible Flow in Complex Geometries on a Massively Parallel Processor, PAM-504, Center for pure and applied mathematics, University of California, Berkeley, California, U.S.A.

Sethian J. A. (1984) Turbulent combustion in open and closed vessels. J. Comp. Phys. 54, 425~456.

Tiemroth E. C. (1986) The simulation of the viscous flow around a cylinder by the random vortex method. Ph. D. Thesis, University of California at Berkeley, California, U.S.A.

Turfus C. (1988) Calculating mean concentrations for steady sources in rectangular wakes by a particle trajectory method. Atmospheric Environment 22(7), 1271~1290.

Wilson D. J. (1982) Estimates of building surface concentrations from nearby point sources. Atmospheric Environment 16(11), 2631~2646.